PROPERTIES OF DARK MANTLES IN LUNAR CRATER ALPHONSUS DEDUCED FROM LROC WAC PHOTOMETRIC MEASUREMENTS. Y. G. Shkuratov[1], V. V. Korokhin[1], M. A. Ivanov[2,3], V. G. Kaydash[1], L. V. Rohacheva[1], G. P. Marchenko[1], and G. Videen[4], [1]Institute of Astronomy, V.N. Karazin National University, 35 Sumska St, Kharkiv, 61022, Ukraine, [2]GEOKHI, Kosygin St., 19, Moscow, [3]Moscow State University of Geodesy and Cartography (MiiGAIK), [4]Space Science Institute, 4750 Walnut St. Suite 205, Boulder CO 80301, USA.

Introduction: The pre-Nectaruian, floor-fractured crater Alphonsus [3,4] (13ºS, 357ºE, 108 km) shows several dark mantles on its floor that usually are interpreted as pyroclastic deposits [1,5,6]. Figure 1 shows a normal albedo map (mosaic) including the crater Alphonsus that was calculated (see below) using several hundreds of individual LROC WAC images acquired at $\lambda = 689$ nm. The crater is optically heterogeneous. In particular, dark mantles are prominent features. We apply LROC WAC data to compare optical roughness [2, 8] of the dark spots with the surrounding areas.

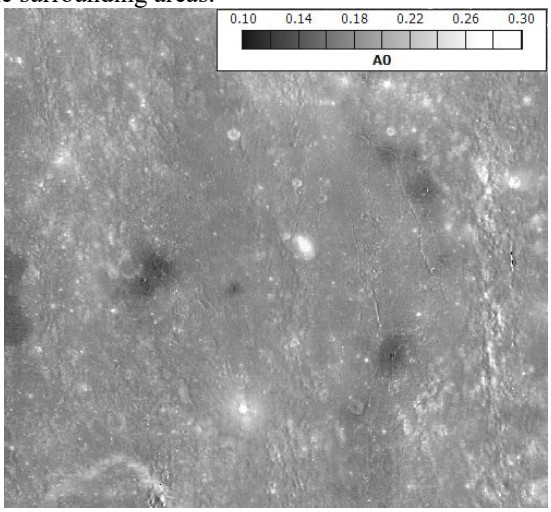

Figure 1. The distribution of the normal albedo A_0

Geology of the crater: Eight material units make up Alphonsus crater (Fig. 2) and its immediate surroundings. Highland materials (undifferentiated, unit **h**) represent the background terrain. To the west of Alphonsus, local to regional lows are filled by mare materials (unit **m**) that represent the eastern edge of the Mare Nubium lava fill. The oldest units inside crater Alphonsus are materials on the wall (unit **wa**) and the floor (unit **fla**) of the crater. Materials on the walls are those of the highlands re-exposed after the Alphonsus impact. Morphologically, materials on the floor are smooth plains. Ejecta from a crater outside of Alphonsus (unit **re**) overlay the medial portion of the Alphonsus floor. The most likely parent crater of the ejecta is crater Arzachel (~100 km in diameter) immediately to the south of Alphonsus. Crater Alphonsus belongs to the class of the floor-fractured craters [3,4]. Graben within crater Alphonsus (unit **g**) are concentrated in the eastern half of the floor where these structures form several N-S-oriented branches. In the southern portion of the floor, graben are oriented in ESE-WMW direction. The graben in their medial parts are ~0.5-1.0 km wide and tens to a few hundred meters deep. Graben cut walls, floor, and remote ejecta materials.

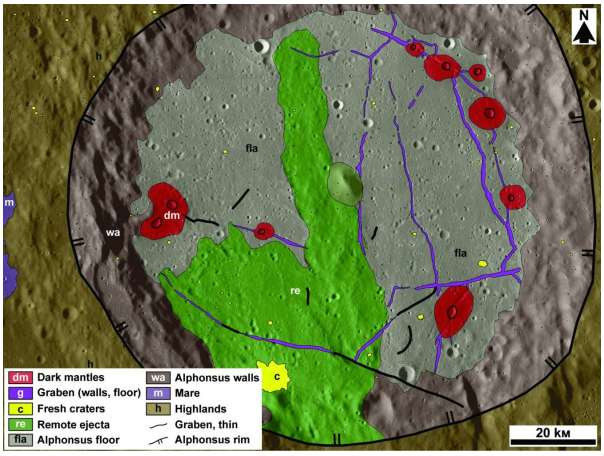

Figure 2. Geological map of the crater Alphonsus

The dark mantling deposits (unit **dm**) with diameters ranging from~3 to 12 km occur on the floor of Alphonsus. All of them are closely associated with the systems of graben and postdate them. Most of the dark deposits are concentrated in the eastern part of the floor (Fig. 2). Circular or slightly elongated depressions usually occur in the center of the dark mantles and likely represent the deposit vents. The mantles have an equidimensional shape that is approximately symmetric relative to the apparent vents. The dark mantling materials are usually interpreted as pyroclastic deposits [1,5,6].

Small (tens of meters to ~2 km in diameter) craters with visually brighter ejecta represent the youngest materials exposed inside and outside of crater Alphonsus. Several tens of small fresher craters occur within the dark mantles. Ejecta from these craters may represent either materials excavated from beneath the mantles or simply less mature, hence brighter, regolith.

Excluding young craters, the Alphonsus floor surface is rather old, since it does not show variations of the parameter OMAT that characterizes the maturity degree of the lunar regolith [7]. In particular, the dark

mantles mentioned above are not seen in the OMAT map shown in Fig. 3.

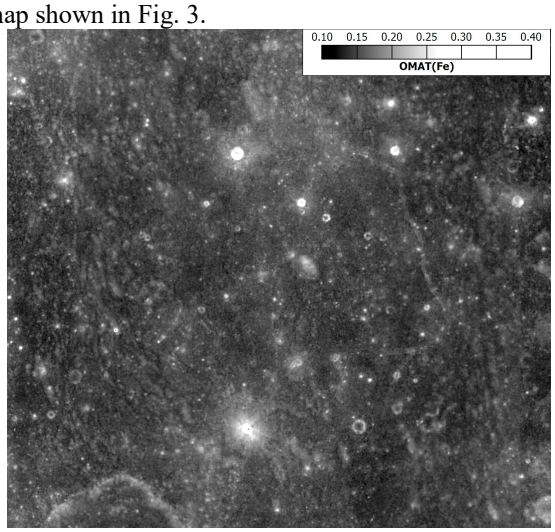

Figure 3. The distribution of the parameter OMAT [7]

Optical roughness: We study Alphonsus using LRO optical measurements to confirm the hypothesis that the dark mantles can be related to pyroclastic deposits. To characterize the optical roughness, we use the following new approximation of lunar phase curves [8]: $A_0 \exp(-\eta\alpha^{\rho})$, where α is the phase angle and the parameters A_0, η, and ρ are, respectively, the normal albedo, total slope and bend of phase curve. These parameters were calculated for each point of the lunar surface in the scene using the mean-square method and tens of LROC WAC images acquired at different phase angles from a range of ~9-80º; the average number of points for the phase-curve approximation is about 140. A detailed description of the processing is presented in [2, 8]. Maps of the parameters are shown in Figs. 1, 4, and 5.

The normal albedo map shows that the crater floor material and surrounding surface have almost the same brightness, which implies equal abundance of chromophore elements such as Fe and Ti (Fig. 1). As can be seen, the map of η demonstrates a very close correlation with A_0 (cf. Figs. 1 and 4). This indicates the total slope of the phase curve depends not only on the surface roughness, but on the albedo as well [9]. Moreover, we found that the parameter η depends also on the wavelength λ. In contrast, the parameter ρ does not depend on λ and very slightly correlates with the albedo [8]. This means that the bend relates to the surface structure. Low values of ρ correspond to areas with higher bend of phase curves. The dark mantles show bent phase curves (Fig. 5). Thus, the surface roughness responsible for the shadows at large phase angles (rock fields), is lower for the dark mantles. This is consistent with the pyroclastic origin of the mantles because the pyroclastic deposits may smooth out the preexisting surface. Unlike the dark mantles, the young craters (Fig. 5) show low bend in spite of the higher albedo. This is because the ejecta of such craters are much rougher than the surrounding terrains.

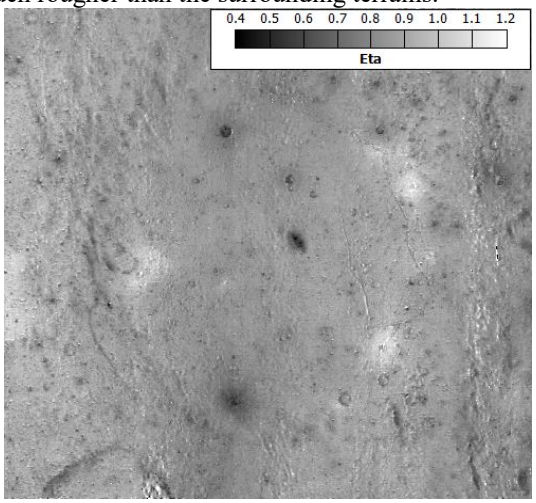

Figure 4. The distribution of the parameter η that describes general slope of phase curves

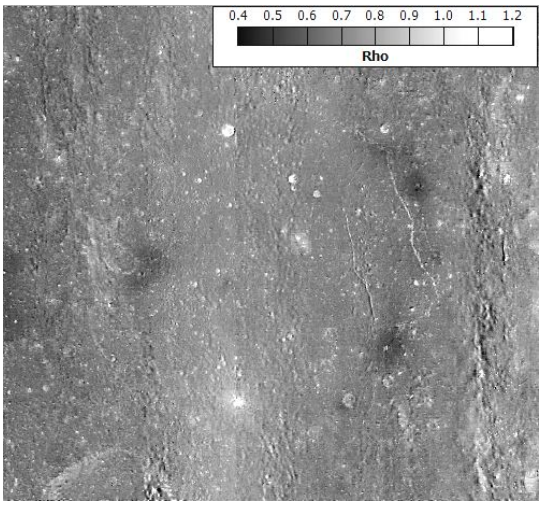

Figure 5. The distribution of the parameter ρ that describes bend of phase curves

References: [1] Head J. and Wilson L. (1979) *Proc. LPSC 10th*, LPI Houston, 2861. [2] Korokhin V. et al. (2014) *PSS*, *92,* 65. [3] Schultz P. (1976) *The Moon* 15, 241. [4] Jozwiak L. et al. (2012) *JGR*, 117, E11005, 2012. [5] Head J. (1974) *Proc. LPSC 5th*, 207. [6] Heiken G. et al. (1974) *GCActa* 38, 1703. [7] Lucey P. et al. (1995) Science, 268, 1150. [8] Korokhin V. et al. (2016) *LPSC 47th*, 1248 (this issue). [9] Hapke B. (1993) *Theory of reflectance and emittance spectroscopy*, Cambridge Univ. Press, 450 p.